LHCb-PUB-2019-007
July 22, 2019

Simulation of light yield attenuation maps for the LHCb SciFi Tracker Upgrade

S. Beranek[1], M. Bieker[2], M. Demmer[2], R. Ekelhof[2], C. O. Gerber[2], M. Whitehead[1], J. Wishahi[2].

[1]*RWTH Aachen University, Aachen, Germany*
[2]*Fakultät Physik, Technische Universität Dortmund, Dortmund, Germany*

Abstract

The Scintillating Fibre (SciFi) Tracker will replace the Inner and Outer Tracker in the LHCb upgrade, to be installed in 2019-2020. It is made from thin scintillating fibres read out by multichannel Silicon Photomultipliers (SiPM). The number of photons reaching the SiPMs depends on the path length of the photons in the fibre and the amount of radiation damage suffered by the fibre. A detailed single fibre simulation in GEANT4 is used to produce maps which give the expected mean light loss for different hit positions in the SciFi detector. The simulation of these maps is described in this note.

Contents

1 Introduction

The LHCb upgrade detector [1] will be installed during 2019 and 2020, prior to data taking in Run 3 of the LHC. The upgrade detector is designed to run at an instantaneous luminosity of 2×10^{33} cm^{-2}s^{-1}, an increase of a factor of five over Runs 1 and 2, collecting an estimated integrated luminosity of $\mathcal{L} = 50\,\text{fb}^{-1}$ by the end of Run 4. This is the default integrated luminosity studied in this note. A core part of the LHCb upgrade project is the Scintillating Fibre (SciFi) Tracker, for full details please see Ref. [2].

The SciFi Tracker is based on 2.5 m long scintillating fibres with a diameter of 250 µm, stacked in six layers with a 275 µm horizontal pitch [2]. The SciFi Tracker is arranged in three stations with four detector layers each, with the two inner layers rotated by $\pm 5°$. The scintillation light is detected by multichannel silicon photomultipliers (SiPM) with a channel width of 250 µm, matching the thickness of the six fibre layers. When a particle crosses the fibres, a signal is generated in more than one corresponding SiPM channel. The hit position is calculated from the charge barycentre. The fibres have a mirror at one end and are read out by SiPMs at the other end. The readout electronics consist of a custom-designed ASIC for pre-amplification, shaping and ADC conversion, and an FPGA for clustering and zero suppression.

A crucial parameter of the SciFi Tracker is the mean number of photons detected by the SiPMs, known as the light yield. The higher the light yield, the lower the probability that the number of photons in a cluster remains below threshold, or in other words the higher the light yield, the higher the hit efficiency. The light yield depends on the energy deposited in the fibres (defined by the number of fibre layers), the number of photons created per unit of energy (the scintillation yield), the attenuation along the fibre, and the photon detection efficiency (PDE) of the SiPMs.

Due to the attenuation of the signal along the fibre the detected light yield is not the same for all hit positions. In addition to the intrinsic attenuation, radiation damage causes the light loss to increase over time. The light yield of irradiated and non-irradiated fibre modules was measured in several test beam campaigns. Nonetheless it is crucial to perform dedicated simulations of the light yield, because the test beam measurements only represent a few single points in space and time.

The attenuation of the light yield along the fibre is a combination of effects from absorption, scattering and reflective losses. For example it depends strongly on the photon wavelength, which then influences the effective PDE. The simulation of the photon transport through the fibre is too complex and computationally time consuming to perform for each event in the LHCb upgrade simulation chain. Therefore a detailed stand-alone simulation has been developed to produce a look-up table, the so-called attenuation map, that gives the relative light yield for hits across the SciFi Tracker detector plane.

The simulation of these attenuation maps is based on the simulation of single fibres (described in Section 3.1), which are combined into maps (Section 3.2) and implemented in the LHCb simulation framework (Section 3.3). It uses a simulation of the expected dose (described in Section 2.1) as input, as well as models for the expected radiation damage as a function of the dose (Section 2.2). The resulting attenuation maps are shown and discussed in Section 4. Systematic uncertainties are presented in Section 5 and comparisons to test beam measurements are reported in Section 6. Finally, Section 7 concludes the note.

2 Inputs

This section describes the inputs and steps required to produce the light yield attenuation maps.

2.1 Dose maps

The input dose maps for the simulation of the light yield attenuation maps are produced for an integrated luminosity of $50\,\text{fb}^{-1}$ at the z coordinates (approximately) 760 - 780 cm, 780 - 800 cm, 900 - 920 cm and 920 - 940 cm with the FLUKA simulation package [3,4]. The dose maps are simulated [5] using the geometry of the current Inner and Outer Tracker [6] for proton–proton collisions at a centre-of-mass energy of 14 TeV. The difference with respect to using the dose deposited in the correct SciFi detector material is expected to be very small. The maps at a z-position of about 8 m correspond to tracking station T1, and those at around 9 m relate to tracking station T3. The maps at the lower z-values are based on the Inner Tracker positions, and the higher ones are based on the Outer Tracker locations.

The dose maps are provided in $2.5\,\text{cm} \times 2.5\,\text{cm}$ bins within 1 m in x and y from the beampipe, and in bins of $20\,\text{cm} \times 20\,\text{cm}$ for the outer region, as shown in Fig. 1. In the coarser regions, linear interpolation is used to obtain a dose map with $2.5\,\text{cm} \times 2.5\,\text{cm}$ granularity, as shown in Fig. 2 for all of the z positions available. The granularity of the FLUKA dose maps defines that for the overall dose maps and the final attenuation maps. It is only necessary to consider one quarter, chosen to be the upper right quadrant, of the SciFi Tracker given the symmetry of the LHCb detector.

The radiation dose shown in Fig. 1 ranges from 0.03 kGy at the outermost corners to 20.60 kGy in the centre, close to the beampipe hole, for $z = 920$ - 940 cm. Comparisons of the available dose maps are shown in Fig. A.1 in Appendix A.

2.2 Radiation damage models

The radiation dose accumulated by the fibres leads to a decrease of the measured light yield during the lifetime of the detector. The average number of photons reaching the photodetectors is driven by two main factors; the number of photons created and the attenuation along the fibre. Previous studies have shown that it is important to perform a specific irradiation campaign with the exact fibre type used in the SciFi Tracker. Irradiation studies using the same fibre type used for the SciFi tracker are introduced in Ref. [2] and studied further in Ref. [7]. The results are briefly described below.

It was found in preliminary studies that the number of photons produced is not harmed by the radiation dose levels relevant for the LHCb upgrade. However, radiation damage of the fibres is seen in terms of a reduction of the transparency due to the formation of absorption centres (localised regions with higher photon absorption). The results of several irradiation tests were combined to define a model to describe the additional attenuation as a function of the wavelength of the photons and the radiation dose applied. From basic principles, it is expected that the damage increases linearly with the dose. However, the data shows that lower damage per dose is seen with higher doses. Saturation of the initial damage is not expected in the radiation dose range considered, but an increased photon yield due to annealing could explain the lower relative damage at high doses. To describe this scenario, a power-law model is used to model to the data, including the decreased rate of damage at high doses. An alternative explanation for the lower relative damage at high doses could be a systematically higher dose rate at these irradiation campaigns. To account for this, a linear model is determined from the low dose rate data and extrapolated to high doses, this is known as the “worst-case model”. In both models the wavelength dependence is described by the same exponential decrease of the damage with increasing wavelength. The resulting functions are

$$a_{\mathrm{r,\,pow}} = 0.4\,D^{0.8}\,\mathrm{e}^{-3.01\times10^{-2}\,(\lambda-450)},$$

$$a_{\mathrm{r,\,lin}} = 0.38\,D\,\mathrm{e}^{-3.01\times10^{-2}\,(\lambda-450)},$$

with the attenuation a given in m^{-1}, the dose D in kGy and the wavelength λ in nm.

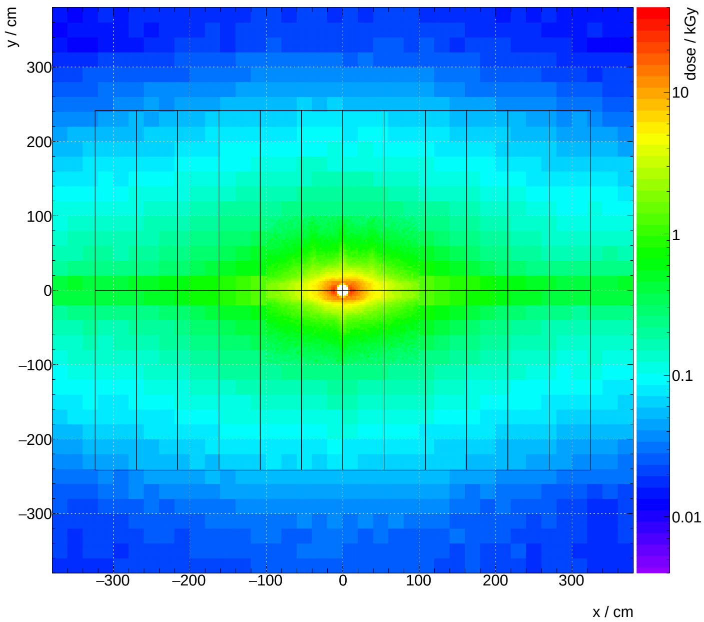

Figure 1: FLUKA dose map in the $x-y$ plane, without interpolation, for $z = 920$ - $940\,\mathrm{cm}$ for $\mathcal{L} = 50\,\mathrm{fb}^{-1}$. The black lines indicate the position of the modules.

The data points and the models are shown in Fig. 3. The power-law model is used as the standard description for the attenuation maps, since it is gives the best description of the available data without underestimating the attenuation. The linear, worst-case, model is used as a conservative alternative to study the case of dose-rate-dependent radiation damage (see Section 5). Neither of the two models can explain all of the differences between the irradiation campaigns, which may be caused by different particle types. It is expected that the uncertainty on the radiation damage is small compared to the difference between these two models. Irradiation campaigns performed with the correct particle mixture and a realistic dose rate did not show systematic differences to the models [7, 8].

3 Implementation

The method used to produce the attenuation maps is split into three parts. Section 3.1 describes the single fibre simulation implemented using GEANT4 [9], where each of these

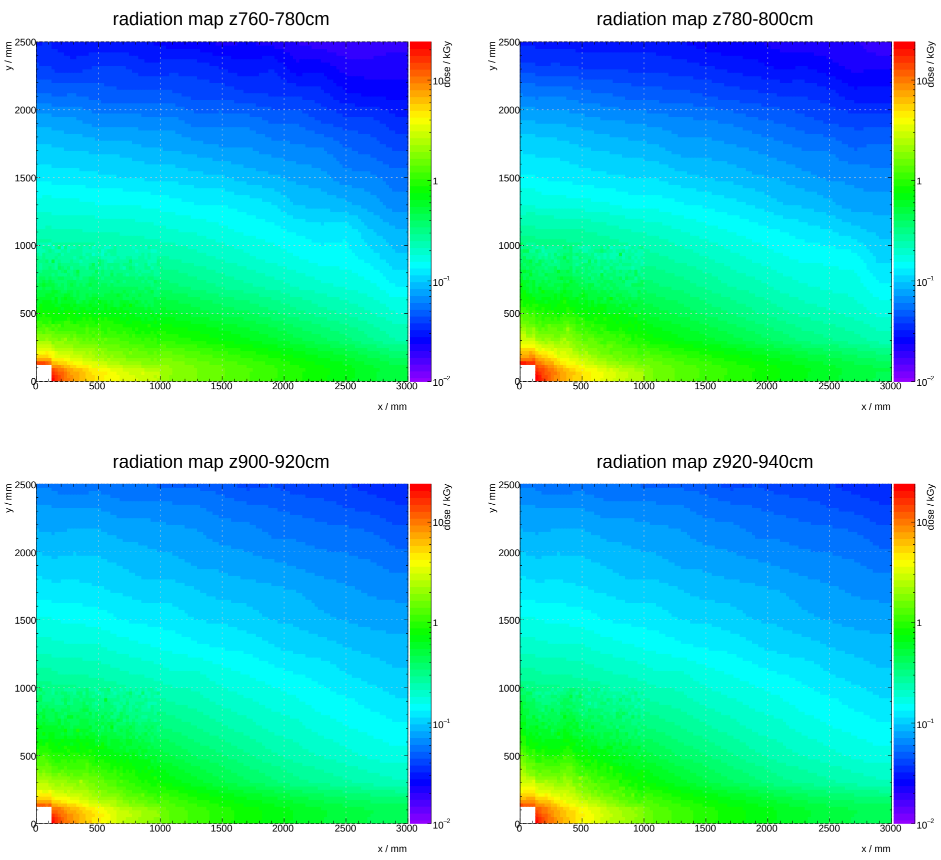

Figure 2: FLUKA dose map in the $x-y$ plane, with interpolation, for (top left) $z = 760$ - 780 cm, (top right) $z = 780$ - 800 cm, (bottom left) $z = 900$ - 920 cm and (bottom right) $z = 920$ - 940 cm for $\mathcal{L} = 50\,\mathrm{fb}^{-1}$ in the upper right quarter of the SciFi Tracker.

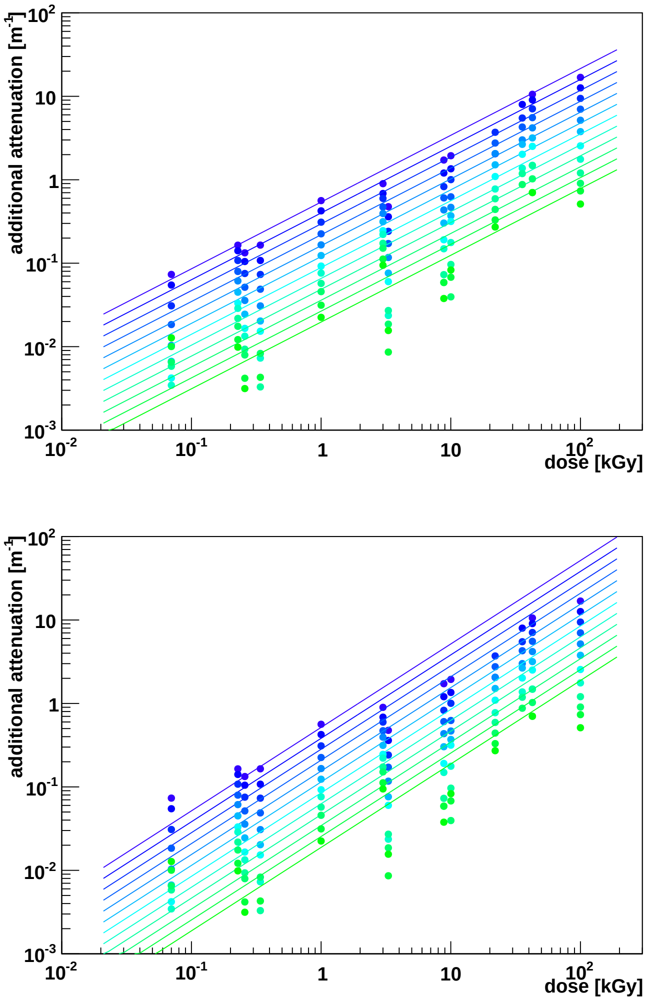

Figure 3: The attenuation data compared to a power-law model (top) and a linear model (bottom) for different wavelengths in 10 nm steps from 440 nm (blue) to 550 nm (green) [7].

simulations fills one bin of the attenuation maps, the production of these maps are described in Section 3.2. Finally, the attenuation maps are stored as xml-files and read in by the LHCb simulation in Boole [10], as explained in Section 3.3.

3.1 Single fibre simulation

A simulation of single scintillating fibres was developed using the GEANT4 framework [11, 12]. The basic geometry used is a round fibre, including two cladding layers, each with a thickness of 3% of the total diameter. The core material is polystyrene and the inner cladding layer is made from polymethyl methacrylate. The outer cladding layer material is described by the manufacturer as a fluorinated polymer, without further details. For the purpose of the simulation poly(trifluoroethyl methacrylate) is used because its refractive index and density match those of the unknown material. The simulated fibre is then placed inside a vacuum, with a mirror at one end and a detector at the other.

The relationship between the attenuation in the fibre and the wavelength is provided by a parameter file. In addition to the basic attenuation, the losses caused by radiation damage are included as a function of the wavelength and the dose, see Section 2.2 for details. The dose profile is taken from the 2D FLUKA dose maps, introduced in Section 2.1.

The basic attenuation within the fibres is simulated using values from literature for pure polystyrene and the wavelength shifter (for more information see Ref. [11]). However, measurements of scintillating fibres used by the LHCb experiment show higher the expected absorption. This can be explained by different effects, such as an additional absorption due to impurities in the core material or by losses at imperfect cladding boundaries during total internal reflection. The latter has a strong effect on the angular dependence of the absorption and can therefore be addressed with the help of dedicated measurements. These are described in Ref. [7].

The scattering and absorption processes of the fibre material are included in the GEANT4 simulation. The losses due to imperfect reflection of the photons at the boundary between the core and the cladding are applied afterwards, since the number of reflections for each photon is stored. This enables the reflection parameter to be adjusted without running a new GEANT4 simulation. An equivalent approach is used for the mirror reflectivity, it is set to 100% during the initial simulation, and a lower reflectivity is applied afterwards, see Section 3.3.

3.2 From single fibre simulations to attenuation maps

The aforementioned GEANT4 single fibre simulation is used to calculate the light yield attenuation by comparing the number of detected photons to the number of generated photons at a given excitation point. In order to obtain a map of attenuation coefficients for different (x, y)-coordinates in the SciFi Tracker, many ($n_{\text{simulations}}$) single fibre simulations are performed. Each simulation corresponds to an excitation with n_{photons} photons produced at this (x, y)-coordinate. The number of detected photons is measured, assuming by default an irradiated SciFi Tracker with an integrated luminosity of 50 fb^{-1}, taking into account the radiation dose profile, given by the 2D FLUKA dose map. To save computing time, the simulation generates the scintillation photons isotropically on a plane inside the fibre core, without simulating an ionising particle that passes through the fibre and produces photons. Simulations that correspond to the same x-coordinate of the dose map can be considered as simulations of an identical fibre with the same dose profile along y but at different excitation points. Therefore the required number of simulations is given by

$$n_{\text{simulations}} = n_{\text{fibres}} \cdot n_{\text{excitations}}$$

with

$$n_{\text{fibres}} = \frac{x_{\text{quarter}}}{x_{\text{bin}}} \text{ and } n_{\text{excitations}} = \frac{l_{\text{fibre}}}{y_{\text{bin}}}.$$

Given the symmetry of the detector, it is sufficient to simulate only one quarter, which results in $x_{\text{quarter}} = 3000\,\text{mm}$. To account for the rectangular beampipe hole of 130.8 mm width and 115 mm height, the fibre length l_{fibre} is 2385 mm for $x \leq 130.8\,\text{mm}$ and 2500 mm for $x > 130.8\,\text{mm}$. With dose map bin sizes of $x_{\text{bin}} = y_{\text{bin}} = 25\,\text{mm}$ this gives

$$n_{\text{simulations}} = 120 \cdot 101 = 12120.$$

In order to ensure the correct radiation-induced attenuation of the photons, the (x, y)-coordinates of the excitation point are positioned in the centre of the lower edge (in y) of a dose map bin, so that on average the correct dose is applied:

$$x_i = 25\,\text{mm}/2 + i \cdot 25\,\text{mm} \quad \text{with} \quad i = 0, 1, 2, \ldots 119$$
$$y_i = 0.5\,\text{mm} + i \cdot 25\,\text{mm} \quad \text{with} \quad i = 0, 1, 2, \ldots 100.$$

As mentioned in Section 3.1, it is possible to change certain parameters like the PDE of the SiPMs or the reflection losses of photons at the core-cladding and cladding-cladding boundaries without having to rerun the simulations. This is because additional information on the produced, wavelength-shifted (WLS) and detected photons from the single fibre simulation is stored, in particular the wavelength distribution and the number of reflections in the fibre. During the calculation of the attenuation coefficients, the number of detected photons is weighted by the reflection efficiency $\varepsilon_{\text{refl}}^{\text{fibre}}$, due to photon losses from core-cladding and cladding-cladding reflections, and the SiPM PDE $\varepsilon_{\text{PDE}}(\lambda_i)$, on an event-by-event basis

$$\varepsilon_{\text{refl}}^{\text{fibre}} = (1 - p_{\text{BL}})^{n_{\text{refl,i}}},$$
$$\varepsilon_{\text{PDE}}(\lambda_i) = p_3(\lambda_i - \lambda_{\max})^3 + p_2(\lambda_i - \lambda_{\max})^2 + \varepsilon_{\text{maxPDE}}.$$

Here, $p_{\text{BL}} = 5 \cdot 10^{-5}$ is the photon loss probability, which is taken from studies with the single fibre GEANT4 simulation, and $n_{\text{refl,i}}$ is the number of reflections at the boundaries core-cladding and cladding-cladding for photon i.

The PDE $\varepsilon_{\text{PDE}}(\lambda_i)$ for the 2017 SiPMs is obtained from a regression of a third-degree polynomial. The parameters are $p_3 = 39.20 \cdot 10^{-9}\,\text{nm}^{-3}$, $p_2 = -12.02 \cdot 10^{-6}\,\text{nm}^{-2}$, $\varepsilon_{\text{maxPDE}} = 0.4216$ and $\lambda_{\max} = 479.1\,\text{nm}$. The results can be seen in Fig. 4, which also shows results from superseded SiPMs.

In summary, a lookup table is produced, containing the light yield attenuation coefficients for every bin of the input dose map for direct and mirror reflected photons:

$$\varepsilon_{\text{direct photons}}(x, y) = \sum_{i}^{N_{\gamma,\text{direct}}} \varepsilon_{\text{refl}}^{\text{fibre}}(x, y) \cdot \varepsilon_{\text{PDE}}(x, y),$$
$$\varepsilon_{\text{reflected photons}}(x, y) = \sum_{i}^{N_{\gamma,\text{refl}}} \varepsilon_{\text{refl}}^{\text{fibre}}(x, y) \cdot \varepsilon_{\text{PDE}}(x, y).$$

3.3 The Boole project

The energy deposited in the SciFi detector by the incident particle is simulated by the `Gauss` application [13] and distributed to different fibres in the `Boole` stage. The attenuation

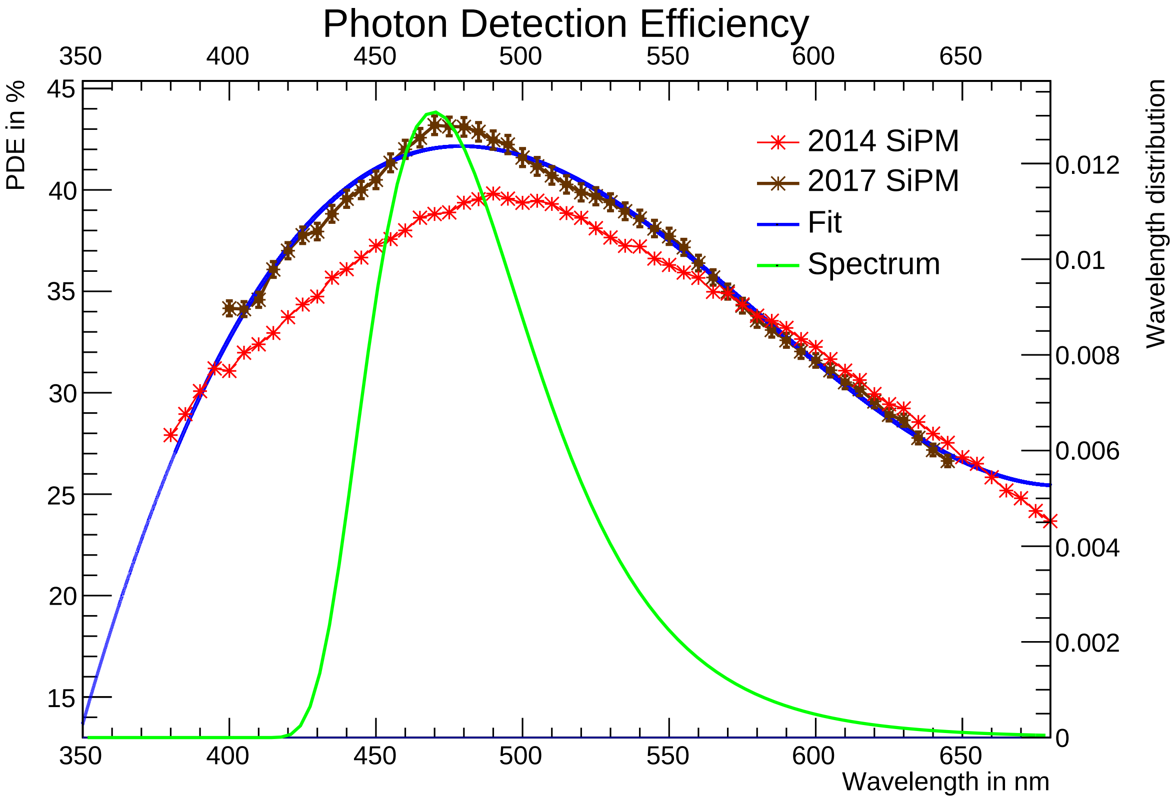

Figure 4: SiPM photon detection efficiency as a function of the wavelength, which is applied in the attenuation maps. The function is a 3rd degree polynomial fitted to data from lab measurements. The red dots correspond to data points from superseded SiPMs.

maps are used within the `Boole` project to convert the energy deposited by an incoming particle into a number of photons that reach the SiPM detector at the end of the fibre. Direct and reflected signals are treated separately and the latter is additionally attenuated by the mirror reflectivity. The energy is then converted to an expected mean number of photons by a global scaling factor which is determined from comparisons to test beam measurements. A random number is drawn from a Poisson distribution for each fibre to get the number of photons seen by the SiPMs for the specific events. Each photon is assigned an arrival time which is used to add the direct and the reflected photons, respecting the time dependent behaviour of the read-out electronics.

The expected number of photons from an interaction, for either direct or reflected phtons, is given by

$$\overline{n}_{\mathrm{dir/refl}} = k \cdot \alpha_{\mathrm{dir/refl}} \cdot E_{\mathrm{hit}}, \tag{1}$$

in terms of the deposited energy E_{hit}, a constant scaling factor k[1], and the attenuation coefficient α for direct or reflected photons. Based on this expected value, $n_{\mathrm{dir/refl}}$, the

[1]This factor is used to tune the overall light yield of the simulation to match the results from test beam measurements.

number of photons is drawn from a Poisson distribution. The attenuation coefficients depend on the position of the hit in the tracker and the values are taken from the corresponding attenuation maps. The absolute values of the coordinates are used because only one quarter of the tracker is directly represented by the attenuation map. No interpolation is performed between the bins of the map.

The attenuation maps, in xml format, are stored in the simulation conditions database, which is used to store parameters required during the simulation of the LHCb (upgrade) detector. The values stored in these databases are static, therefore multiple irradiation maps are stored in the database corresponding to non-irradiated fibres and for irradiated fibres with integrated luminosities of $1\,\mathrm{fb}^{-1}$, $10\,\mathrm{fb}^{-1}$, $25\,\mathrm{fb}^{-1}$, $50\,\mathrm{fb}^{-1}$ (default) and $100\,\mathrm{fb}^{-1}$. The attenuation map can be simply selected by options passed to the `Boole` software. The xml-file for the attenuation map includes information about the bin layout and the values of the attenuation coefficients in each bin. Two arrays containing the bin edges are used to describe the location of the bins and two more arrays for the two attenuation coefficients stored per bin, representing the values for direct and reflected photons. The arrays of attenuation coefficients are produced by flattening the two-dimensional histograms of the attenuation maps. In the area of the beampipe hole the values of the attenuation coefficients are set to zero. The bins above the beampipe at 100.5 mm are filled by the excitation points at 115.5 mm.

4 Results

The light yield attenuation maps show the number of photons detected by the SiPMs divided by the number of generated photons for hits across the SciFi detector planes. The value is the product of the efficiency of photons being caught by the wavelength shifter, the trapping efficiency of the "shifted" photons in the fibre, the attenuation along the fibre and the PDE of the SiPMs.

The light yield attenuation maps for no irradiation, corresponding to $0\,\mathrm{fb}^{-1}$, are shown in Fig. 5 for direct and reflected photons and their sum. The combined attenuation maps assume an equal weight for both the direct and reflected photons and are for illustration only, the simulation ultimately considers direct and reflected photons separately in the `Boole` step as discussed in Section 3.3. The combined values for reflected and direct photons range from 0.019 in the centre right beside the beampipe hole (137.5 mm in x and 25 mm in y) to 0.036 at the upper edge of the detector (12.5 mm in x and 2500 mm in y).

The light yield attenuation maps using the power-law radiation damage model, as described in Section 2.2, for a radiation dose corresponding to $50\,\mathrm{fb}^{-1}$ are shown in Fig. 6 for direct and reflected photons and their sum. The combined values for reflected and direct photons range from 0.012 in the centre right beside the beampipe hole (137.5 mm in x and 25 mm in y) to 0.036 at the upper edge of the detector (2612.5 mm in x and 2500 mm in y). These represent the nominal results.

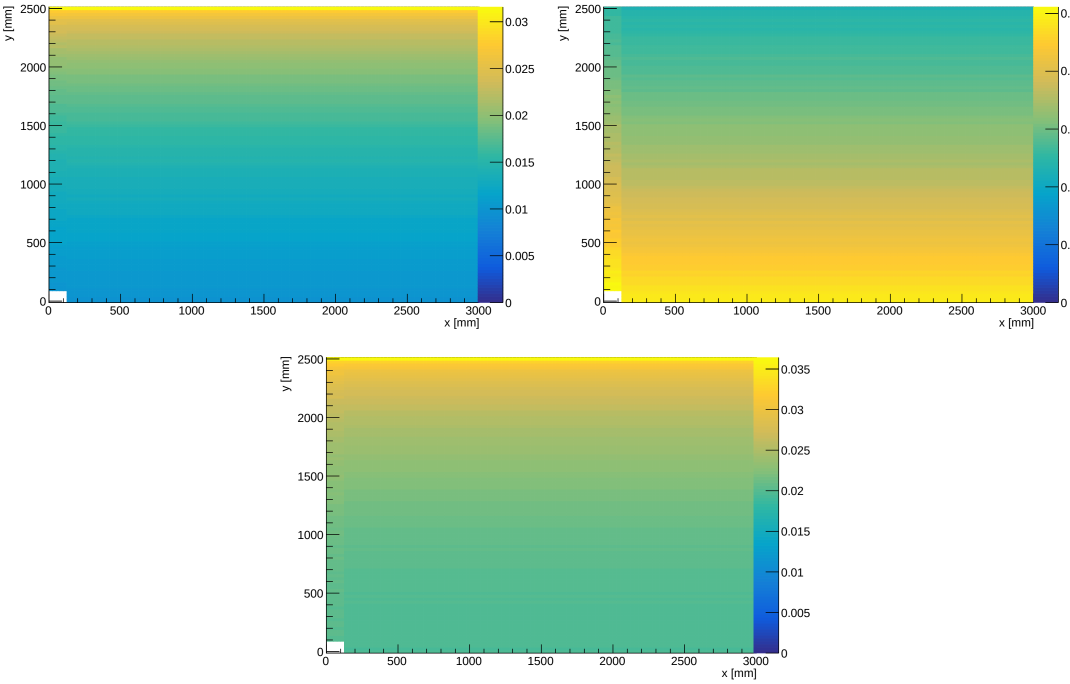

Figure 5: Light yield attenuation maps for no radiation ($\mathcal{L} = 0\,\text{fb}^{-1}$) for (top left) direct photons, (top right) reflected photons and (bottom) both combined, in the upper right quarter of the SciFi Tracker.

5 Systematic uncertainties

The different sources of systematic uncertainties associated with the production of the attenuation maps are studied in this section.

5.1 Doubled dose

The nominal dose accumulated from collecting a data sample corresponding to $50\,\text{fb}^{-1}$ is increased to that for a $100\,\text{fb}^{-1}$ data sample. This is considered for several reasons, firstly because this is given as an uncertainty on the FLUKA maps themselves, and secondly because the experiment may run longer or accumulate luminosity more quickly than expected. The effect of using a doubled dose in the input FLUKA maps can be found in Fig. 7. A projection of bins 6 ($x = 125 - 150\,\text{mm}$) and 120 ($x = 2975 - 3000\,\text{mm}$) are also shown. The variations for direct photons range from $-2.0\,\%$ to $23.3\,\%$ and for reflected photons from $3.6\,\%$ to $32.9\,\%$ with respect to the light yield attenuation map using the default single dose. Systematic uncertainties for reflected and direct photons combined range from $-0.1\,\%$ at $x = 1562.5\,\text{mm}$ and $y = 2450\,\text{mm}$ to $23.7\,\%$ at $x = 137.5\,\text{mm}$ and $y = 25.0\,\text{mm}$. Here, and subsequently, a positive change represents a lower light yield compared to the default map.

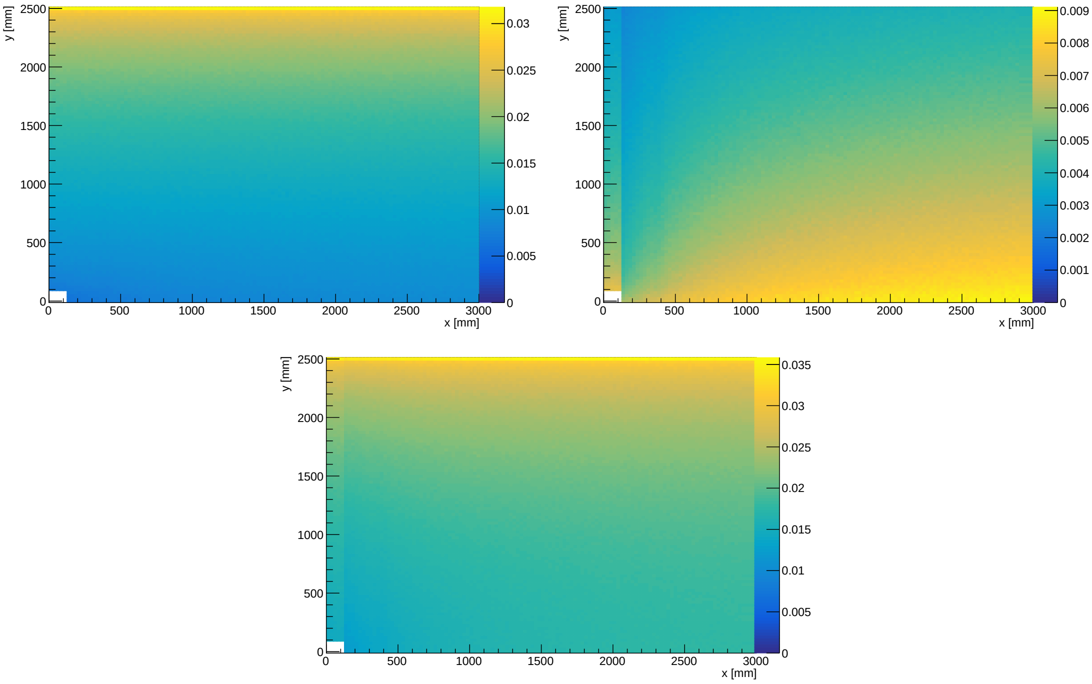

Figure 6: Light yield attenuation map for $\mathcal{L} = 50\,\text{fb}^{-1}$ at z = 920 - 940 cm for (top left) direct photons, (top left) reflected photons and (bottom) both combined, in the upper right quarter of the SciFi Tracker.

5.2 Radiation damage model

The systematic uncertainty due to the choice of the radiation damage model is evaluated by considering the linear model, as described in Section 2.2. The results are shown in Fig. 8. The uncertainties for direct photons range from $-7.0\,\%$ to $10.5\,\%$ and for reflected photons from $-12.0\,\%$ to $19.1\,\%$ with respect to the light yield attenuation map using a power-law radiation damage model (default). The systematic uncertainties for reflected and direct photons combined range from $-6.4\,\%$ at $x = 1687.5\,\text{mm}$ and $y = 275\,\text{mm}$ to $11.7\,\%$ at $x = 137.5\,\text{mm}$ and $y = 0.0\,\text{mm}$.

5.3 Double dose and linear radiation damage model

The systematic uncertainty using a doubled dose in the input FLUKA maps and the linear radiation damage model can be found in Fig. 9. The uncertainties for direct photons range from $-2.8\,\%$ to $39.4\,\%$ and for reflected photons from $0.6\,\%$ to $51.1\,\%$ with respect to the light yield attenuation map using a power-law radiation damage model and the single default dose. The systematic uncertainties for reflected and direct photons combined range from $-1.2\,\%$ at $x = 2637.5\,\text{mm}$ and $y = 2225\,\text{mm}$ to $40.7\,\%$ at $x = 137.5\,\text{mm}$ and $y = 0.0\,\text{mm}$.

A summary of the discussed systematic uncertainties for all photons combined (with a mirror reflectivity of 75%) can be found in Fig. 10 where projections in bin 6 ($x = 125 - 150\,\text{mm}$) (left) and bin 120 ($x = 2975 - 3000\,\text{mm}$) (right) are given.

5.4 Choice of binning

The bin sizes of the dose maps are $x_{\text{bin}} = y_{\text{bin}} = 25\,\text{mm}$ (see Section 2.1 for details). To confirm that this choice of binning is reasonable, the bin with the highest dose gradient is examined. This corresponds to the bin with the highest dose due to the approximately exponential behaviour of the radiation. This bin and all bins at the same x position, which contain the same fibres, are called the "worst case bin". They contain the full-length fibres which are most affected by radiation. As shown in Fig. 11, the worst case bin is located next to the beampipe hole and the lower four bins therefore have no neighbours on the

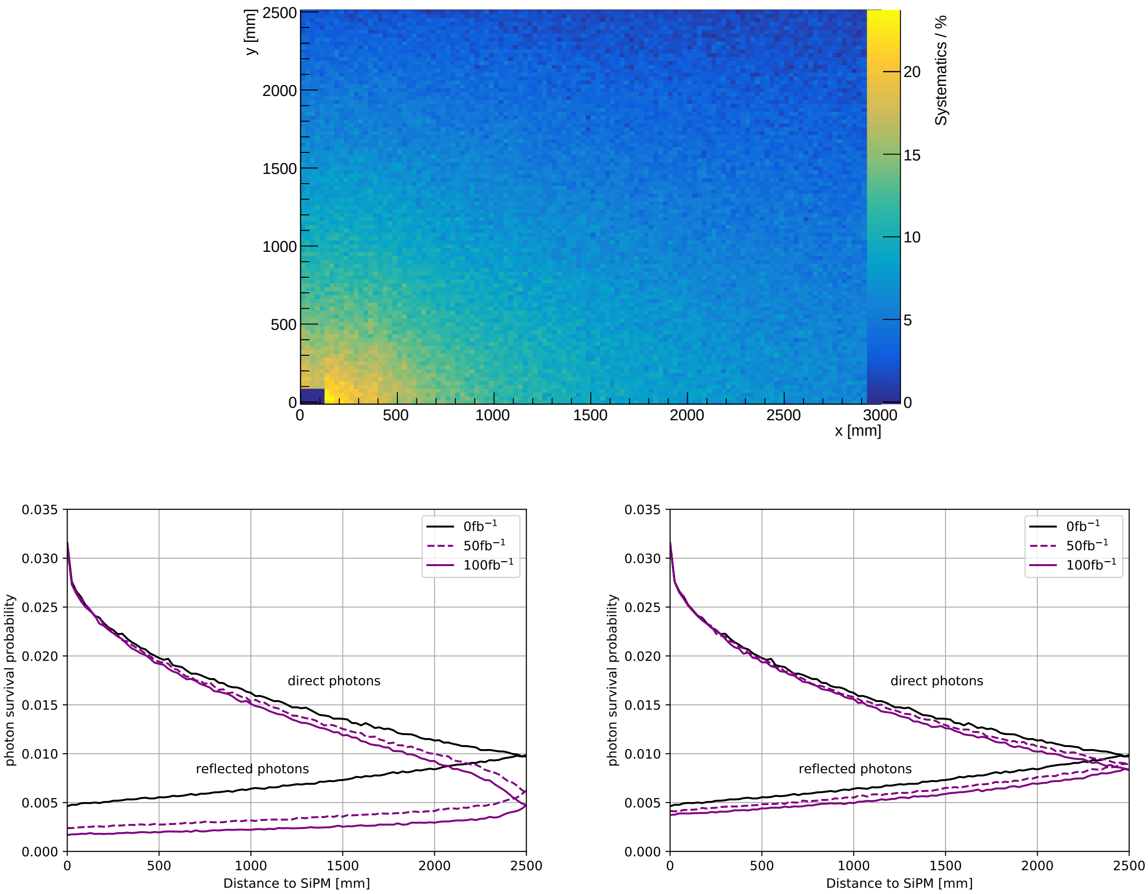

Figure 7: The effect of using a doubled dose with respect to the default dose in the input FLUKA maps for the light yield attenuation map at $z = 920 - 940\,\text{cm}$ for $\mathcal{L} = 50\,\text{fb}^{-1}$ for (top) direct and reflected photons combined in the upper right quarter of the SciFi Tracker. Projections in bin 6 ($x = 125 - 150\,\text{mm}$) (bottom left) and bin 120 ($x = 2975 - 3000\,\text{mm}$) (bottom right) are also shown.

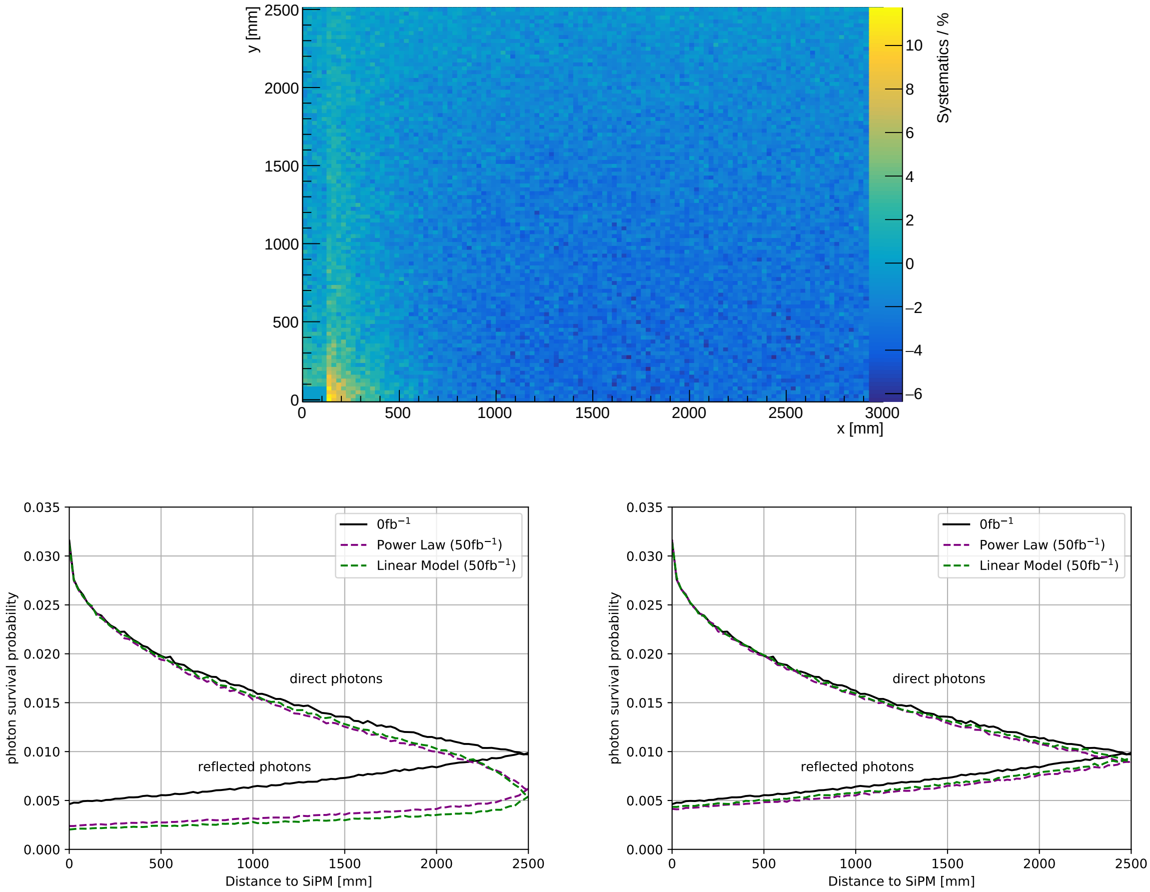

Figure 8: Systematic uncertainties using a linear radiation damage model in the input FLUKA maps for the light yield attenuation map at $z = 920 - 940\,\text{cm}$ for $\mathcal{L} = 50\,\text{fb}^{-1}$ for (top) direct and reflected photons combined in the upper right quarter of the SciFi Tracker. Projections in bin 6 (x = 125 - 150 mm) (bottom left) and bin 120 ($x = 2975 - 3000\,\text{mm}$) (bottom right) are also shown.

left side. For all other bins the deviation of the bin value can be estimated by looking at the value of the adjacent bins.

If the binning is fine enough, the dose profile of the worst case bin should be similar to that of the most affected fibre within the same bin ("worst case fibre"). As shown in Fig. 11, the worst case fibre is located on the very edge of the worst case bin. Interpolation between the worst case bin and the adjacent bins to the left is used to determine the radiation dose profile of the worst case fibre. The initial FLUKA dose map does not include the beam-pipe hole and so contains values for the missing region, which makes such an interpolation possible. The mean dose of the worst case fibre is 4 % and the peak dose is 14 % higher than the dose of the worst case bin. The single fibre simulation shows that for an excitation at the end of the fibre, the light yield fraction compared to an non-irradiated fibre is 61.99 % for the worst case bin and 61.55 % for the worst case fibre.

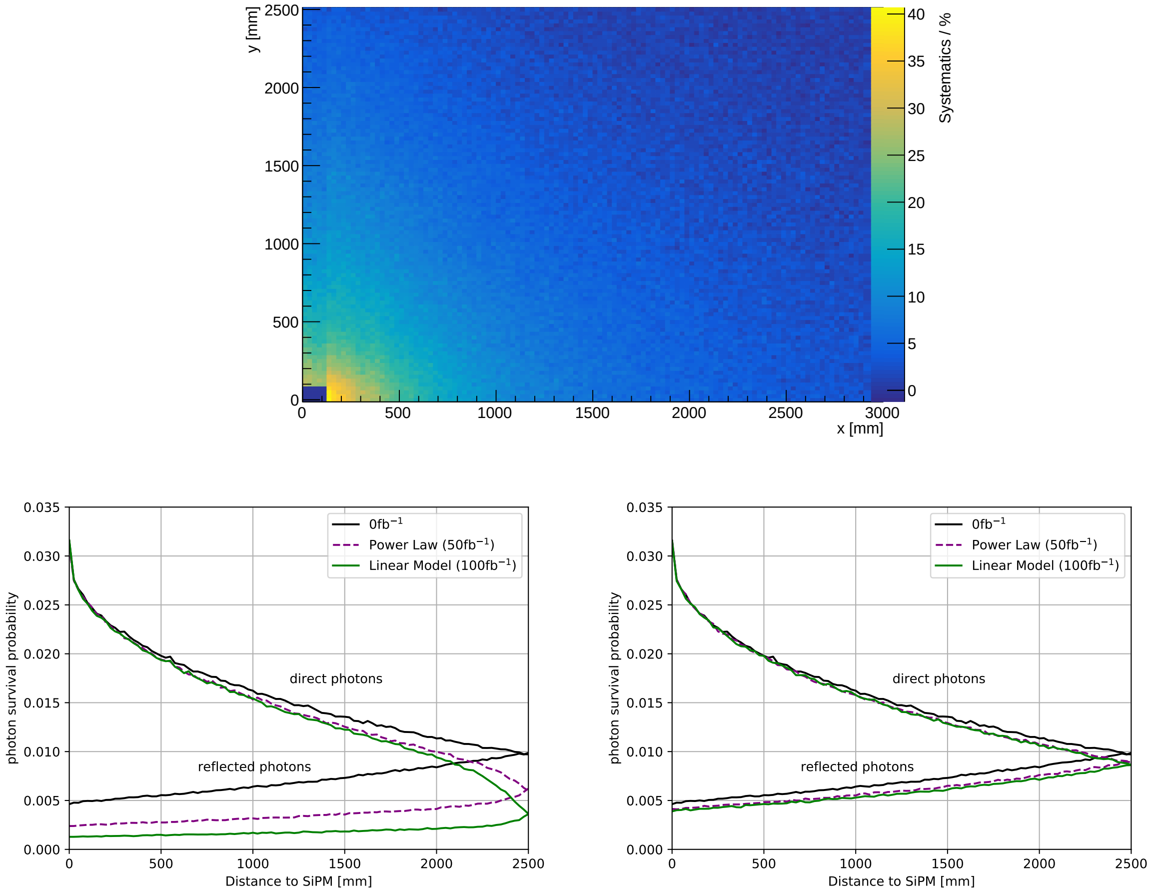

Figure 9: Systematic uncertainties using a doubled dose in the input FLUKA maps and the linear radiation damage model for the light yield attenuation map at $z = 920 - 940\,\text{cm}$ for (top) direct and reflected photons combined in the upper right quarter of the SciFi Tracker. Projections in bin 6 ($x = 125 - 150\,\text{mm}$) (bottom left) and bin 120 ($x = 2975 - 3000\,\text{mm}$) (bottom right) are also shown, with a comparison to the default attenuation (power law model, $\mathcal{L} = 50\,\text{fb}^{-1}$).

Since the worst case fibre and worse case bin differ by less than 0.5 %, the bin size is found to be sufficient.

6 Comparison to measurements

This section compares the simulated results with data from real fibre mats.

6.1 Comparison of initial attenuation

To assess the validity of the simulated light yields they are compared to measurements of real fibre mats. The light yield of 200 mats were measured at four different points during the mat production process. The four positions (A-D) are 2230 mm, 1430 mm, 815 mm

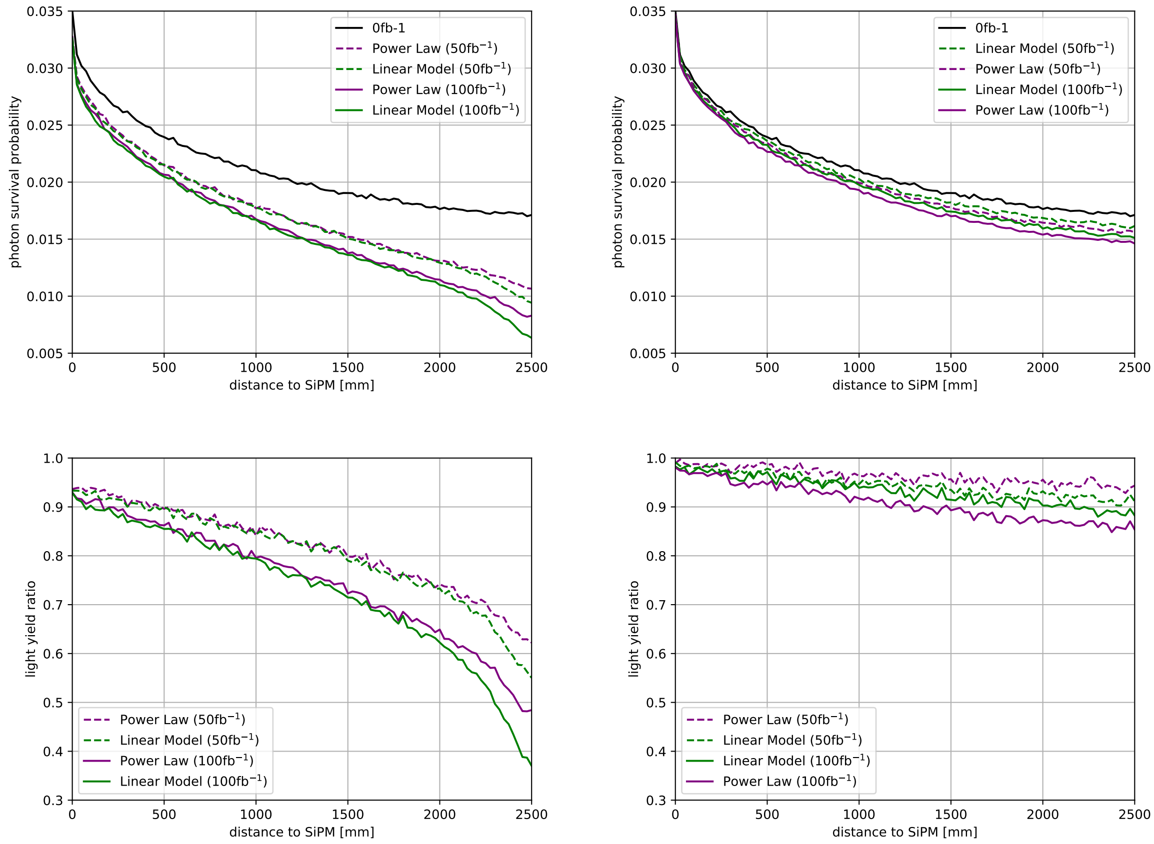

Bin 6 ($x = 125 - 150\,\mathrm{mm}$) Bin 120 ($x = 2975 - 3000\,\mathrm{mm}$)

Figure 10: The upper plots show values of the maps for three different irradiation levels and the two damage models. The lower plots show the ratio with respect to the values of the $\mathcal{L} = 0\,\mathrm{fb}^{-1}$ (no radiation) maps. A projection in bin 6 ($x = 125 - 150\,\mathrm{mm}$) (left column) and bin 120 ($x = 2975 - 3000\,\mathrm{mm}$) (right column) is shown.

and 205 mm away from the SiPMs. For each of the four measurement points the mean value is calculated. The uncertainty at each point is given by the width of the light yield distribution of all mats. The mirror reflectivity in the simulation is set to 75 %, which is comparable to measurements. The simulated distribution is scaled to the measurement point closest to the mirror (point A) in data. This is motivated by the fact that the light yield of the simulated detector is also scaled to test beam results at this position. The comparisons between simulation and data are shown in Fig. 12, where the simulation shows good agreement with the measurement results within their uncertainties.

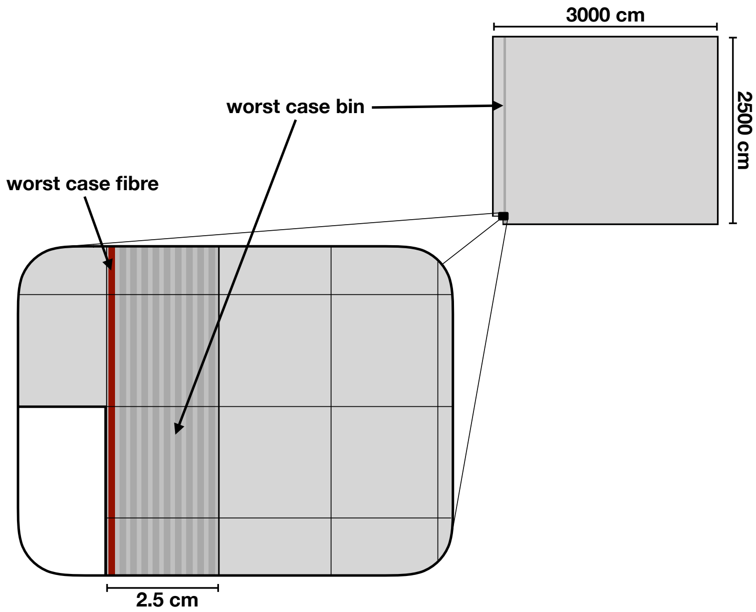

Figure 11: The bins at the same x-position right next to the beampipe hole, which contain fibres with the full length of the detector, are called “the worst case bin”. This bin consists of the most irradiated fibres. The fibre most affected by radiation is located on the very edge of this bin and is called “the worst case fibre”.

6.2 Comparison of simulated and irradiated mats

The simulation is also assessed by comparing the attenuation of irradiated fibres implemented in the simulation to those from an irradiated mat. The dose profile for the measurement was chosen to match the dose profile of the worst case bin [14]. The results are shown in Fig. 13, where decent agreement is seen between data and simulation over the range of hit positions.

Measurements of the irradiated mat before, and 35 days after, irradiation [15] are shown in Fig. 14. The power law model is used due to the high dose rate during the irradiation process. The simulated light yield of the non-irradiated mat is scaled to the data points 2230 mm away from the SiPM (Point A in Fig. 12). Good agreement is seen between the light yields for the non-irradiated maps, while the simulation slightly overestimates the light yield for the irradiated map.

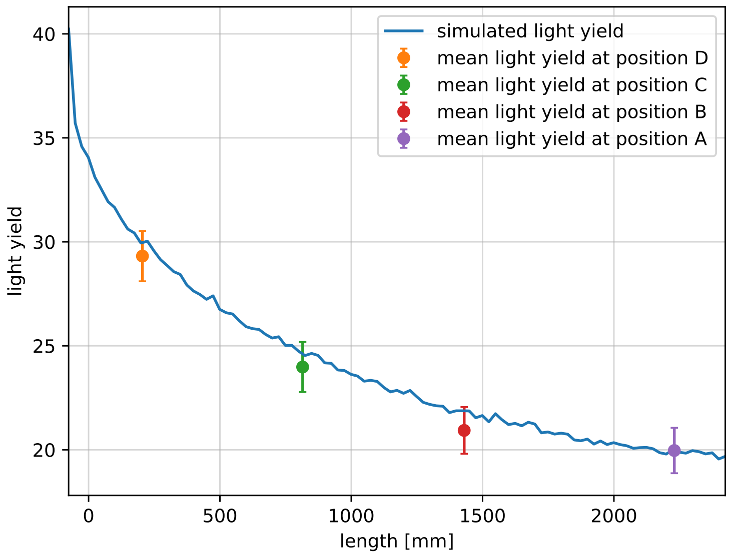

Figure 12: A comparison between the simulated light yield and the measured light yield of fibre mats. The simulated values are scaled to match the data at point A.

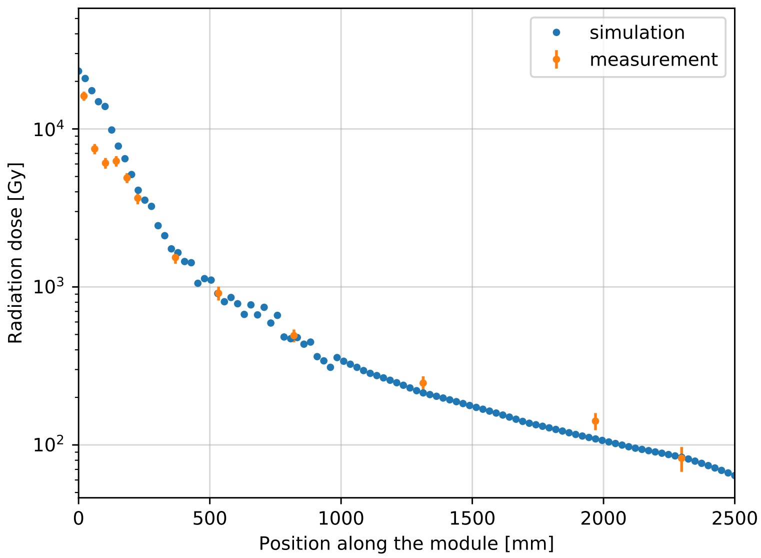

Figure 13: The dose profile of the irradiated mat in data (orange) and simulation of the worst case bin (blue) [14].

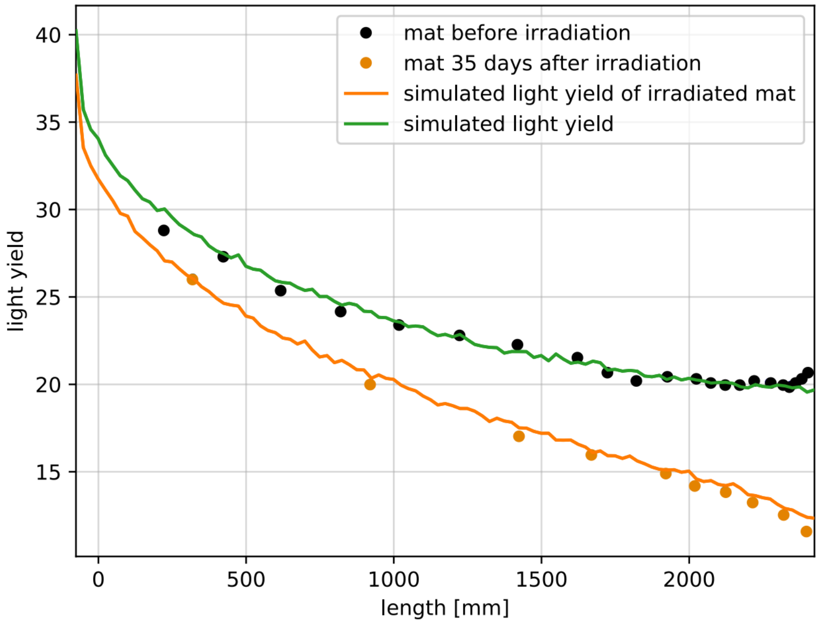

Figure 14: Measured light yield of a mat before (dark blue) and after irradiation (light blue) compared to simulations. Simulations are scaled to point A of the measured light yield before irradiation (2230 mm away from the SiPM) [15].

7 Conclusion

The expected number of photons seen by the photodetectors is a crucial number for the performance of the SciFi Tracker, which is being installed during Long Shutdown 2 of the LHC. The degradation of the photon signal due to radiation damage is a complex process requiring detailed simulations that are too computationally time consuming to be performed for every event of the LHCb detector simulation.

The expected dose profile and radiation damage model are used in a single fibre GEANT4 simulation to determine the attenuation of the photon signal along the fibre between the hit position and the SiPMs. Tens of thousands of single fibre simulations are performed to build the light yield attenuation maps, which are then used as look-up tables in the LHCb detector simulation.

The expected change of the light yield for different detector lifetimes and radiation damage models can be simulated. The light yield attenuation maps show the expected behaviour. The overall attenuation values are dominated by the trapping efficiencies of the photons in the fibres, which are a only few percent. The dependence on the position is given by the attenuation in the fibres. This is lowest for those areas close to the beampipe for the irradiated maps, since the high particle density in the forward direction provides the highest dose, and therefore the most radiation damage, in this region. The reduction of the light yield close to the beampipe is around 35 % after 50 fb^{-1} which matches the expectation from earlier simulations and measurements.

An alternative model is tested to study the influence of a possible dose rate dependence of the radiation damage. This linear model shows a reduction of the light yield of up to 12 % compared to the default model.

Additional attenuation maps are simulated that can be used to study the effect of different radiation doses, corresponding to integrated luminosities of 0 fb^{-1}, 1 fb^{-1}, 10 fb^{-1}, 25 fb^{-1}, 50 fb^{-1} and 100 fb^{-1}. The worst case scenario is described by the combination of a doubled dose and the linear radiation damage model. The ratio of this worst case scenario and the detector before irradiation shows a 40 % decrease in the light yield for the area close to the beampipe.

The resulting values of the attenuation maps are based on the single fibre simulation which are tuned to measurements of single fibres. Comparisons between simulation and actual measurements show that the values for the non-irradiated case agree well with the measurements of 240 mats performed during the course of the production. The region most effected by irradiation is compared to a dedicated fibre mat which was irradiated with the corresponding dose profile and the results agree within the uncertainties.

The inclusion of the attenuation maps in the LHCb detector simulation is an important step towards providing realistic simulated data samples in the LHCb upgrade era. Additionally, it will allow studies of the tracking efficiency as a function of the radiation damage to be performed.

A Appendix

A.1 Fluka dose maps

Figure A.1 shows the FLUKA dose maps for the nominal $\mathcal{L} = 50\,\text{fb}^{-1}$ at z positions 780 - 800 cm , 900 - 920 cm and 920 - 940 cm as a ratio with the $z = 760$ - 780 cm map. As expected, on average the dose in the downstream stations decreases with distance. This is especially pronounced in the low y region, whereas detector acceptance effects lead to an increased dose at large values of y.

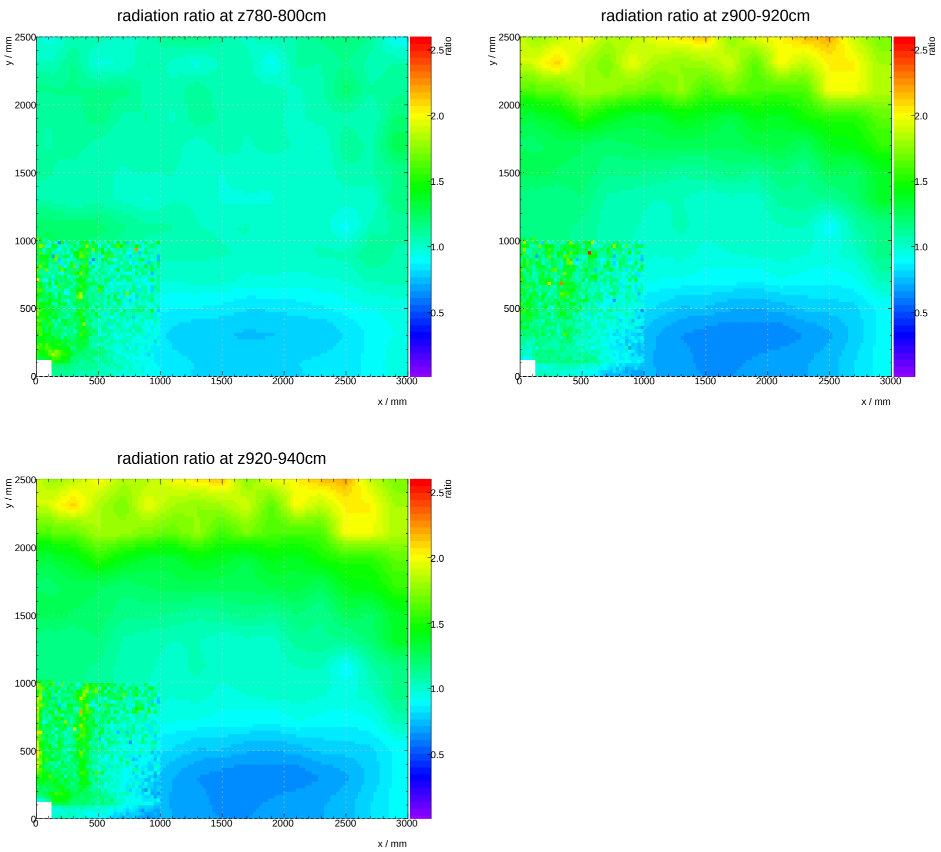

Figure A.1: FLUKA dose map with interpolation as a ratio with respect to $z = 760$ - 780 cm. $z = 780$ - 800 cm (top left), $z = 900$ - 920 cm (top right) and $z = 920$ - 940 cm (bottom) for $\mathcal{L} = 50\,\text{fb}^{-1}$ in the upper right quarter of the SciFi tracker.

References

[1] LHCb collaboration, *Framework TDR for the LHCb Upgrade: Technical Design Report*, CERN-LHCC-2012-007. LHCb-TDR-012.

[2] LHCb collaboration, *LHCb Tracker Upgrade Technical Design Report*, CERN-LHCC-2014-001. LHCb-TDR-015.

[3] T. T. Böhlen *et al.*, *The FLUKA Code: Developments and Challenges for High Energy and Medical Applications*, Nucl. Data Sheets **120** (2014) 211.

[4] A. Ferrari, P. R. Sala, A. Fasso, and J. Ranft, *FLUKA: A multi-particle transport code (Program version 2005)*, CERN-2005-010 (2005) .

[5] M. Karacson, *Evaluation of the Radiation Environment of the LHCb Experiment*, PhD thesis, TU Vienna, 2016, CERN-THESIS-2016-246.

[6] LHCb, A. A. Alves, Jr. *et al.*, *The LHCb Detector at the LHC*, JINST **3** (2008) S08005.

[7] R. Ekelhof, *Studies for the LHCb SciFi Tracker – Development of modules from scintillating fibres and tests of their radiation hardness*, PhD thesis, TU Dortmund, 2016, CERN-THESIS-2017-098.

[8] J. Menne, *The LHCb SciFi Tracker: studies on scintillating fibres and development of quality assurance procedures for the SciFi serial production*, PhD thesis, TU Dortmund, 2018, https://eldorado.tu-dortmund.de/handle/2003/36869.

[9] GEANT4, S. Agostinelli *et al.*, *GEANT4: A Simulation toolkit*, Nucl. Instrum. Meth. **A506** (2003) 250.

[10] `http://lhcbdoc.web.cern.ch/lhcbdoc/boole`.

[11] M. Deckenhoff, *Scintillating Fibre and Silicon Photomultiplier Studies for the LHCb Upgrade*, PhD thesis, TU Dortmund, 2015, CERN-THESIS-2015-318.

[12] Bieker, M. , Ekelhof, R. and Manderfeld, R. , *Description of Light Guidance in Dual Clad Scintillating Fibres for the LHCb SciFi Tracker*, LHCb-PUB-2019-006.

[13] M. Clemencic *et al.*, *The LHCb Simulation Application, Gauss: Design, Evolution and Experience*, Journal of Physics: Conference Series **331** (2011), no. 3 032023.

[14] L. Gavardi, *Studies for the LHCb SciFi Tracker – Investigation of SCSF-78 scintillating fibres performances and development of a novel class of highly efficient scintillating fibres*, PhD thesis, TU Dortmund, 2017, TU Dortmund PHD Thesis.

[15] D. Müller, *Performance studies of irradiated scintillating fibre modules and quality checks during serial production for the LHCb SciFi Tracker*, Master's thesis, University of Heidelberg, 2017. Uni Heidelberg Master Thesis.